Universiteit
Leiden
The Netherlands

Making it big : how characean algae use cytoplasmic streaming to enhance transport in giant cells

Meent, J.W. van de

Citation
Meent, J. W. van de. (2010, September 16). *Making it big : how characean algae use cytoplasmic streaming to enhance transport in giant cells. Casimir PhD Series*. Retrieved from https://hdl.handle.net/1887/15949

Version:	Corrected Publisher's Version
License:	Licence agreement concerning inclusion of doctoral thesis in the Institutional Repository of the University of Leiden
Downloaded from:	https://hdl.handle.net/1887/15949

Note: To cite this publication please use the final published version (if applicable).

1 CELL SIZE, DIFFUSION AND TRANSPORT

Living organisms show a remarkable variation in sizes, yet the dimensions of a typical cell are surprisingly similar across species. In nearly all plant-like multicellulars the constituent cells measure 10-100 μm. Animal cells, whilst generally somewhat lesser in size to their plant counterparts fall into a similar range. Single-cellular prokaryotes are yet smaller, with bacteria like *E. coli* weighing in at just over 1 μm and 0.2 μm accepted as the lower size limit of cellular life. Thus outside of a few notable exceptions the overwhelming majority of organisms have cell sizes in the range 1-100 μm. One of the big open questions in biology is what underlying mechanism has determined the evolution of this relatively well-conserved length scale.

The fact that very few cells are larger than 100 μm suggests that this typical size may reflect physical constraints, such as the diffusive range over which two metabolites can be reliably expected to interact. In this context the outliers that do show larger cell sizes provide key counterexamples, prompting the question in what way these species have managed to compensate for any problems associated with an increasing cell size, and what utility this design provides in an evolutionary context.

In some cases large sizes are found in cells with a highly specialised role. The nerve fibres in our body can reach lengths of several feet. An extreme example is the *giant squid axon*, that can have a diameter up to 1 mm, improving the propagation speed of their action potentials which ultimately facilitates a faster escape response. In other cases, single-cellular organisms have evolved to a large size and complexity. Examples of this are the protozoa *Paramecium*, which can reach sizes of 350 μm, and the trumpet-shaped *Stentor* which can be as large as 2 mm. Arguably even more developed is the algae *Acetabularia*, a single-cellular organism that grows into a plant-like stalk that can be as long as 10 cm. Finally there are the characean algae, a family of plant-like weeds whose segmented stems are built up out of cylindrical *internodal cells* of 200-1000 μm diameter and lengths that can exceed 10 cm.

What the cells in the above examples have in common is that they each show active forms of internal transport, driven by the movement of *molecular* motors along intracellular filaments that make up the *cytoskeleton*. This motion is often called *trafficking* when it involves targeted transport of individual organelles and vesicles. If this motion results in a continuous circulation of the cellular fluid, it is called *Cytoplasmic streaming*, or

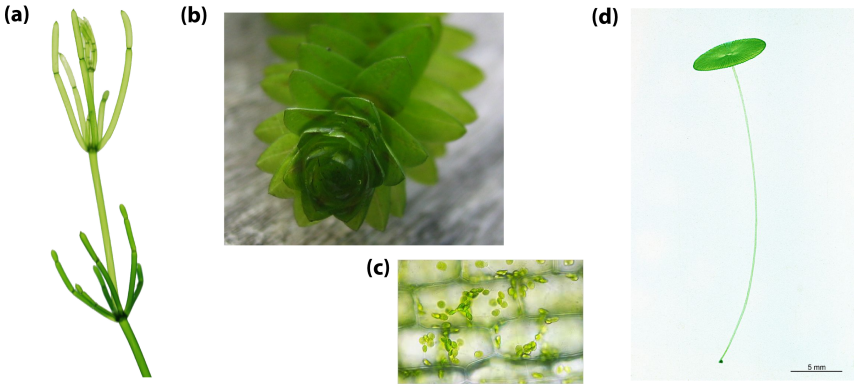

Figure 1.1 Examples of species exhibiting cytoplasmic streaming. **(a)** Chara **(b)** Elodea **(c)** Micrograph of cells in an Elodea leaf **(d)** Acetabularia.

sometimes also *cyclosis*. Streaming is found in many types of larger eukaryotic cells, particularly in plants. Patterns of circulation take various shapes and can be very steady. Cytoplasmic streaming has long been conjectured to aid in overcoming the slowness of diffusion on long length scales, thereby increasing internal mixing and aiding the cell's ability to maintain *homoeostasis*, the stable supply of metabolites under fluctuating levels of uptake and demand.

The central objective of our research on this subject is to quantify fluid dynamical aspects of this form of circulation and elucidate its role in enhancing metabolic rates, ultimately developing an understanding of how streaming may help overcome the physical limits associated with large cell sizes.

This project has been a collaborative undertaking between Leiden University, where the author has been supervised by Wim van Saarloos and the lab of Ray Goldstein at the University of Cambridge, where a large part of the work presented in this thesis was carried out. A number of collaborators have been involved at various stages of this project. They are Idan Tuval, Marco Polin, Cyril Picard, Andy Sederman and Vasily Kantsler.

1.1 Cytoplasmic Streaming in Green Algae and Higher Plants

Cytoplasmic streaming as a phenomenon has been known for more than two centuries, with the first observations attributed to the work of Bonaventura Corti in 1774. It occurs in a range of cell types and is found in a

variety of organisms including amoebae, protozoa, fungi and slime molds, though most commonly in plants and their highest genetic predecessors, the *Characean algae* (see reviews by Kamiya (1959, 1962, 1981) as well as Allen and Allen (1978a,b)).

In the case of the latter two, a large corpus of research over the last 5 decades has established that streaming results from the action of *myosin* motor proteins. These molecular motors attach to organelles, particles and vesicles pull these structures along tracks of actin filaments, entraining the cytoplasm (for an overview, see Shimmen (2007) as well as Shimmen and Yokota (2004)). Actin is a polar filament, along which myosin moves in a well-defined direction. The form of circulation that arises is therefore determined by the topology of the actin network.

Though the mechanics underlying cytoplasmic streaming have been studied extensively, there is relatively little insight as to its biological function. A number of authors, most notably Pickard, have suggested that streaming may serve to enhance metabolic rates in large cells, where timescales for diffusion become prohibitively large (Pickard, 1974, 2003; Hochachka, 1999). The central objective of this research is to make these ideas specific, by focusing on fluid dynamical aspects of streaming, combining modelling with modern experimental techniques such as PIV, microrheology and NMR based velocimetry.

In a wider context, it is becoming more and more apparent that many transport processes in cells require explanation (Hochachka, 1999; Agutter et al., 2000; Agutter and Wheatley, 2000). In the past, a simplified picture of a cell as a watery bag of enzymes has often been invoked for lack of a more detailed model. This metaphor is now making way for the notion of the cytoplasm as an environment that is both highly crowded and highly structured. Thermal motion is often sub-diffusive (Banks and Fradin, 2005; Golding and Cox, 2006) and the cytoskeleton has being implicated in various forms of targeted transport (Dinh et al., 2006; Snider et al., 2004; Maly, 2002; Smith and Simmons, 2001). Our work on cytoplasmic streaming can in this sense be seen as part of a broader effort to understand the interplay between spatial and biochemical aspects of cellular metabolism.

Cytoplasmic streaming is customarily classified into two major groups. The term *amoeboid* streaming is used to denote forms cytoplasmic motion that induce changes in cell form, the best known of which is probably *shuttle streaming* found in slime molds (Kamiya, 1959, 1981; Allen and Allen, 1978b). Our focus here is on non-amoeboid streaming, which is generally

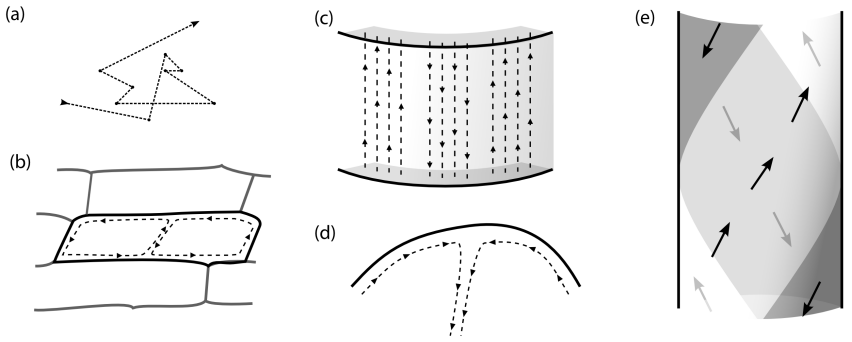

Figure 1.2 Schematic illustrations of streaming topologies. **(a)** Saltation **(b)** Circulation **(c)** Reverse-fountain streaming **(d)** Multistriate streaming **(e)** Rotational streaming.

divided into 5 classes based on visually apparent phenomenology, as originally identified by Kamiya (1959) (see also Allen and Allen (1978a) and Pickard (2003)). The best studied by far of these is the *rotational streaming* found in characeans, which is the subject of this thesis and will be reviewed in detail in the next chapter. Other forms of streaming commonly identified are *saltation*, *circulation*, *fountain streaming* and *multistriate streaming*. We will briefly describe each of these patterns of circulation.

- *Saltation*, sometimes also known as *glitschbewegung* or *agitation*, is the most widespread form of cytoplasmic movement (Kamiya, 1959; Allen and Allen, 1978a), characterised by apparently random jumps of cytoplasmic particles over distances much larger than those corresponding to thermal fluctuations. Displacements can be as large as 100 μm. Microtubules are possibly implicated in this form of streaming, since very active saltation is observed near spindles, within centrosomes and adjacent to microtubular organelles (Allen and Allen, 1978a).

- *Circulation* takes the form of movement along the cell wall and strands of cytoplasm transecting the vacuole. Circulation patterns are typically stable on the timescale of minutes, and evolve as transvacuolar strands move and branch. Both unidirectional and bidirectional movement are known and velocities can be as large as 40 µm/s. Cells exhibiting circulation include hair cells in various plants such as *Urtica* (stinging nettle), and parenchymal (i.e. bulk) cells in *Allium* (the onion genus), as well as the leaf cells of the water plant *Elodea* (Kamiya, 1959; Allen and Allen, 1978a).

- *Fountain streaming* is circulation where the cytoplasm moves along a central axis, flowing back in the opposite direction along the cell wall. *Reverse-fountain* streaming exhibits an inward motion along the central axis and is the more common of the two (Kamiya, 1962; Allen and Allen, 1978a). In some cell types it is a developmental stage towards rotational streaming. True fountain streaming is typically found in pollen tubes of various plants.

- *Multistriate streaming* is found in the fungus *Phycomyces* and in the marine algae *Acetabularia*. The cells of Acetabulria have a cylindrical stalk that is several centimetres in length, containing a large vacuole separated by a tonoplast from a thin layer of *cytoplasm*, at the periphery. Streaming occurs in both directions along channels separated by stationary cytoplasm (Allen and Allen, 1978a). Some forms of circulation could arguably be seen as multistriate streaming, such in the marine algae *Caulpera*, where streaming forms 100 μm wide bands wherein files of chloroplasts stream bidirectionally in a circadian rhythm (Allen and Allen, 1978a).

1.2 Flow and Diffusional Limits at the Cellular Scale

To understand how these types of circulation processes might help overcome the limits of diffusion at large length scales, we will first take some time to explore the basic dynamics that govern flows and diffusive transport around microorganisms. As E.M. Purcell famously observed in his paper *Life at Low Reynolds Numbers* (1977), diffusion and fluid motion behave in ways that are often contrary to physical intuition when examined at the cellular scale. A fundamental property of flows in this regime is that inertia plays no role. Moreover the diffusive motion of individual molecules is relatively large compared to typical displacements.

To understand the physical constraints that microscopic organisms have to contend with, we will discuss the implications of both these concepts in a little further detail. Let us start by examining what it means to have a fluid where inertia plays no role. The flow field $\boldsymbol{v}$ of a liquid with constant density ρ must satisfy two basic equations. The first is that the velocity field $\boldsymbol{v}$ has a zero divergence everywhere:

$$\nabla \cdot \boldsymbol{v} = 0 \, . \tag{1.1}$$

This ensures that no mass can accumulate at any point in space, thereby fulfilling the condition that the density of the fluid is constant. Given this

requirement, the balance of forces is then given by a second equation:

$$\rho\left(\frac{\partial \boldsymbol{v}}{\partial t} + \boldsymbol{v}\cdot\nabla\boldsymbol{v}\right) = -\nabla p + \eta\nabla^2\boldsymbol{v}\,. \tag{1.2}$$

The term $(\partial_t \boldsymbol{v}+\boldsymbol{v}\cdot\nabla\boldsymbol{v})$ has dimensions $[\mathrm{m/s}^2]$ and can be interpreted as the local acceleration in the advective frame of the flow, sometimes known as the acceleration in a *Lagrangian* frame. The left hand side of the equation therefore takes the form of a mass density times an acceleration and can be interpreted as the *force per volume* associated with this acceleration. The right hand of the equation gives the force density associated with the pressure gradients ∇p and the viscous drag $\eta\nabla^2\boldsymbol{v}$. The parameter η that determines the magnitude of the drag term is known as the *viscosity* of the fluid.

The relative strength of each of these terms can be examined by writing the equations in their *dimensionless* form. For any problem we can choose a typical scale V for the velocity variations we are interested in, as well as a typical length R over which the velocity field varies significantly. Using these two typical values, we can rescale the coordinates, velocity and pressure as:

$$\boldsymbol{r} = R\tilde{\boldsymbol{r}}\,, \qquad \boldsymbol{v} = V\tilde{\boldsymbol{v}}\,, \qquad t = \frac{R}{V}\tilde{t}\,, \qquad p = \frac{\eta V}{R}\tilde{p}\,. \tag{1.3}$$

After this substitution, the derivatives map to

$$\nabla = \frac{1}{R}\tilde{\nabla}\,, \qquad \frac{\partial}{\partial t} = \frac{V}{R}\frac{\partial}{\partial \tilde{t}}\,. \tag{1.4}$$

Equation (1.2) then takes the form

$$\mathrm{Re}\left(\frac{\partial \tilde{\boldsymbol{v}}}{\partial \tilde{t}} + \tilde{\boldsymbol{v}}\cdot\tilde{\nabla}\tilde{\boldsymbol{v}}\right) = -\tilde{\nabla}\tilde{p} + \tilde{\nabla}^2\tilde{\boldsymbol{v}}\,, \qquad \mathrm{Re} = \frac{\rho V R}{\eta}\,. \tag{1.5}$$

In this dimensionless form, all terms in the equation should be expected to be order one, since they have been renormalised with respect to their typical values. The only exception is the dimensionless ratio Re. This parameter, which is known as the *Reynolds number*, determines the relative strength of the acceleration term with respect to the rest of the equation. It increases with the typical velocity and length scale, and decreases with the viscosity.

Let us take a moment to interpret the implications of this result. The above equation tells us that any flow problem in an incompressible fluid to

which a well-defined scale can be assigned is *fully* determined by a single dimensionless parameter Re, no matter how large or small an object, and regardless of the viscous properties of the fluid it moves in. For example, if we want to study the flow around a new ship we have designed, we can build a model to a scale of 1 : 100 and compensate by increasing the flow speed by a factor 100. Since Re only depends on the product of V and R, the flow field around the model should be *exactly* the same as the flow field around the full sized ship, aside from two trivial scaling factors R and V.

The Reynolds number also tells us how flows will change in nature as we approach microscopic scales. The viscosity of an incompressible fluid is often expressed as the ratio $\nu = \eta/\rho$, a quantity known as the *kinematic viscosity*. For water, it lies around 10^{-6} m^2/s, or 10^6 μm^2/s. A human swimmer has a velocity around 1 m/s, and would therefore have a Reynolds number of order Re = 10^6. On the other hand, a bacterium 1 μm in size, swimming at 10 μm/s, would have a Reynolds number of order Re = 10^{-5}. Thus flows on a human scale are inertia dominated, whereas flows on a microscopic scale are almost entirely viscous.

What this means is that microorganisms inhabit a completely different regime of fluid mechanics, where our intuitions shaped by life in a high Re world do not apply. When we swim, we gain momentum by effectively 'pushing' ourselves off with our stroke and subsequently glide through the water during recovery. For a bacterium, the coasting length after the end of a stroke is about 0.1 Å (Purcell, 1977). Movement at microscopic scales is therefore essentially inertia free: all displacements are an instantaneous response to movements of the organism.

This means that if you are not careful about how you swim, you might end up exactly where you started at the beginning of the stroke. An example often quoted in this context is the swimming technique of a scallop, which propels itself by quickly shutting its shell, squirting out a jet of water. At a zero Reynolds number this stroke would just not work, as the scallop would push itself forward when closing, but then precisely reverse its motion when opening up again.

In a mathematical sense this regime is the limit where the flow field adjusts *adiabatically* to a change in boundary conditions. When Re = 0 equation (1.5) reduces to

$$0 = -\tilde{\nabla}\tilde{p} + \tilde{\nabla}^2\tilde{\boldsymbol{v}}\,. \tag{1.6}$$

This form, often called the *Stokes Flow* equations, is linear and therefore reversible in time, since a reverse motion is mathematically be equivalent

to a mapping $t \mapsto -t$ and $\boldsymbol{v} \mapsto -\boldsymbol{v}$. Any type of motion similar to that of the scallop, which is characterised by a *reciprocal* motion where the recovery is simply the reverse of the stroke, will therefore lead to no net displacement.

This reversibility also has fundamental implications for spreading of nutrients. In our world of high Re flows, stirring of a fluid induces turbulence and irreversible mixing. Think of stirring milk into a glass of tea for example. Stirring clockwise and then counterclockwise will not return the fluid to its previous unmixed state. This is very different for Stokes flows as was famously illustrated by Taylor (1966). If a drop of dye is placed in a highly viscous fluid that is then deformed by shear, it can be stretched out until it is no longer visible to the naked eye. Yet if the shearing motion is reversed, the drop will return its original form.

For a microorganism looking for food, life in a low Re world differs significantly from that at macroscopic length scales. Aside from the fact that it needs to adjust its swimming technique and lives in an environment where mixing is largely reversible, a bacterium also needs to contend with the fact that the diffusive motions of the molecules that surround it easily dominate over its own movement. One might suppose that a bacterium swims to improve its nutrient uptake, much in the way a whale swims through water to pick up plankton. However at scales of individual cells this strategy is not necessarily productive.

To see why this is true, we will make a rough estimate for how much swimming could improve nutrient uptake at small scales. The diffusion of a solute in the presence of a flow is described by the so-called *advection-diffusion equation*

$$\partial_t \rho + (\boldsymbol{v} \cdot \nabla)\rho \; = D\nabla^2 \rho. \tag{1.7}$$

Let us calculate the nutrient flux into *E. coli*, assuming for the sake of mathematical convenience that this bacterium is a perfect sphere of radius R in an environment with nutrient concentration ρ_0. We will also assume that *E. coli* is able to extract all nutrients near its surface. In other words, the surface of the sphere is a *perfect sink* that maintains concentration $\rho = 0$. This sink will create a depletion layer around the surface of the cell. Assuming for the moment that there is no flow, the concentration around the organism will only be a function of the radial coordinate r, so the steady-state concentration profile will be determined by the equation:

$$0 = \nabla^2 \rho = \frac{1}{r^2}\frac{\partial}{\partial r}\left(r^2 \frac{\partial \rho}{\partial r}\right) \quad \rightarrow \quad \rho(r) = \frac{A}{r} + B\,. \tag{1.8}$$

Given that $\rho(0) = 0$ and $\rho(\infty) = \rho_0$, the concentration profile around the cell must therefore take the form:

$$\rho(r) = \rho_0 \left(1 - R/r\right) \ . \tag{1.9}$$

The diffusive flux F_{diff} into the cell under these conditions is

$$F_{\text{diff}} = D\nabla\rho = D \left.\frac{\partial\rho}{\partial r}\right|_{r=R} = \frac{D\rho_0}{R} \ . \tag{1.10}$$

Now for a bacterium moving at velocity V, an upper bound for the advective flux is given by

$$F_{\text{adv}} = \rho_0 V \ . \tag{1.11}$$

The relative strength of these two contributions is

$$F_{\text{adv}}/F_{\text{diff}} = VR/D \tag{1.12}$$

E. coli swims at about 30 μm/s and let's say that its radius is 1 μm. Typical small molecules have a diffusion constant of about 1000 $\mu m^2/s$. We see that the relative strength of the advective to diffusive flux is about

$$F_{\text{adv}}/F_{\text{diff}} = 0.03 \ . \tag{1.13}$$

Of course this analysis is highly simplified, since it is based on upper bounds for both fluxes. In order to treat this problem in a more precise manner, we would have to solve the actual advection-diffusion problem.

As is the case with the hydrodynamic equations, we can rescale the advection-diffusion equation with respect to a typical length R and velocity V. The resulting dimensionless is parametrised by a single dimensionless ratio known as the Péclet number

$$\partial_{\tilde{t}}\rho + \text{Pe}(\tilde{\boldsymbol{v}} \cdot \tilde{\nabla})\rho = \tilde{\nabla}^2\rho, \qquad \text{Pe} = VR/D. \tag{1.14}$$

The Péclet number is precisely equal to the ratio $F_{\text{adv}}/F_{\text{diff}}$ we just derived, built up of a typical velocity, length and diffusion constant. When it is small, diffusive fluxes dominate and when it is large advective fluxes are strongest.

So it turns out bacteria do not only live a life at a low Reynolds number, they also live in a world where the Péclet number is small. We will discuss

the effect of flow on diffusion further in the next section. But the conclusion we can draw for microscopic organisms is that swimming should not be expected to increase nutrient uptake significantly. Basically, if you are *E. coli*, then waiting around for your food to *come to you* is essentially as efficient as swimming around to get it.

It was this observation by Purcell (1977) that lead him to hypothesize that *E. coli* does not swim around to extract more nutrients from its environment. Rather, it swims to discover an environment more rich in nutrients. Measurements by Berg and Brown (1972) showed that *E. coli* movements follow a pattern that has now become known as *run and tumble*. The organism swims straight for a while, then randomly reorients itself and then sets off in a different direction, resulting in a trajectory that is much like a random walk. Purcell found a simple argument to estimate how far *E. coli* would have to travel in order for this type of movement to be useful. The time it takes to travel a distance l by swimming is l/v. On the other hand, the time it takes for molecules in the solute to diffuse over the same distance is l^2/D. Thus the typical length at which swimming becomes more important than diffusion is $l = D/v \sim 30$ μm. As it turns out, this length was in fact reasonably close to the typical run distance of *E. coli*.

This result was hugely influential in that it lead to a realisation in the biophysics community that many forms behaviour at the cellular scale can be understood in of the basic physical limits that organisms have to contend with. As we shall see in the next section, analogous types of analysis can be performed for organisms of increasing size. It is in this regime that the strength of the flow around the organism starts to play a key role.

1.3 Life at High Péclet Numbers

In order for organims to increase the rate at which they can extract nutrients from their environment they can either increase their size or their typical swimming velocity. Since Pe and Re both depend on RV, these adaptations will raise both the Péclet and the Reynolds number of the flows around it. However, since D typically has values of 1000 $\mu m^2/s$ or less, whereas $\eta/\rho \simeq 10^6$ $\mu m^2/s$. The Péclet number will therefore become significant before the Reynolds number does as the size of an organism increases.

An example of how the Péclet number can affect nutrient uptake is found in the *Volvocales* (figure 1.3), which have been studied previously

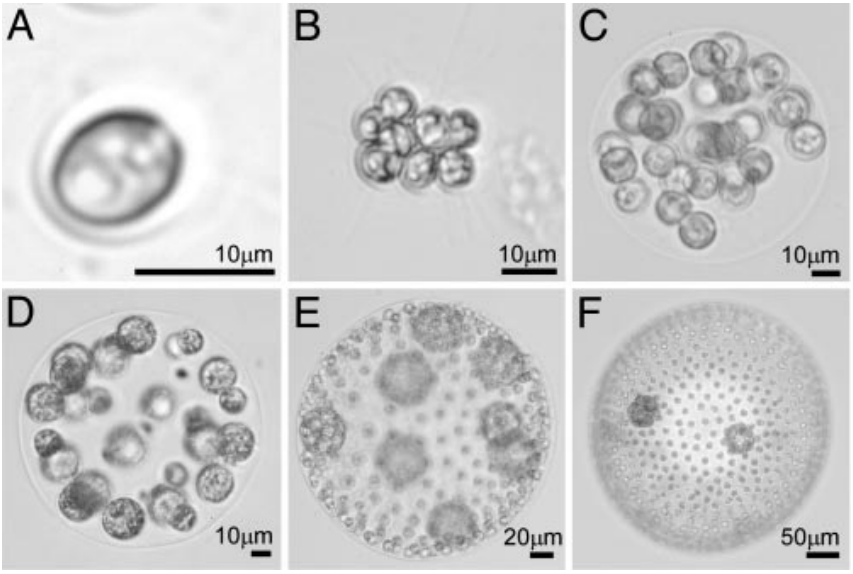

Figure 1.3 Members of the Volvocales as shown by Solari et al. (2006). Species in this family of colonial algae are found in a range of sizes increasing from 1 to 2000 cells. **(a)** The single-cellular *Chlamydomonas reinhardtii* **(b)** *Gonium pectorale* (8 cells) **(c)** *Eudorina elegans* (32 cells) **(d)** *Pleodorina californica* (64 cells) **(e)** *Volvox carteri* (~ 1000 cells) **(f)** *Volvox aureus* (~ 2000 cells).

in our group at Cambridge (Short et al., 2006; Solari et al., 2006). These closely related green algae present an ideal case for the study of the relation between size and nutrient uptake, since they are found in a range of sizes increasing from 10 μm to over 1000 μm.

The smallest member of the family is *Chlamydomonas*, a single-cellular organism that swims using two flagella beating in a form of breast stroke. Other species undergo a number of cell divisions, forming colonies whose number of cells increases with powers of two. In the larger members, these cells organise on a spherical *extracellular matrix*, orienting their two flagella outward to propel the organism. As the size increases further, species start to show differentiation between two types of cells. The *somatic* cells remain on the surface for propulsion, but inside the colony specialised *germ* cells form *daughter colonies* that hatch from the mother once they have matured. This process takes place over a well-defined life cycle that takes places over 48 hours if growth is synchronised in 16/8 hour light-dark cycle (Solari et al., 2006).

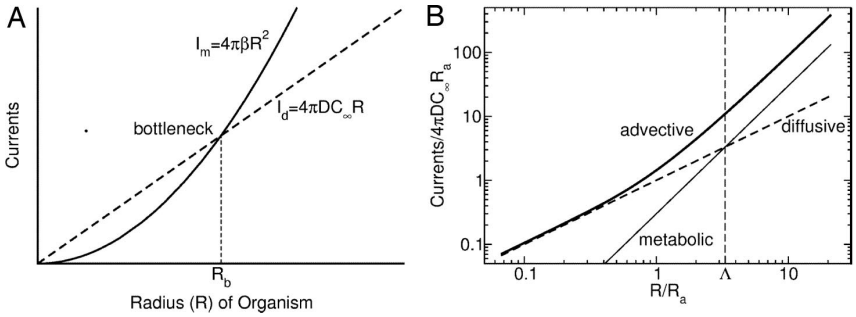

Figure 1.4 Nutrient requirements vs diffusive uptake in the *Volvocales* as presented by Short et al. (2006) **(a)** Since the number of cells increases with the surface area of the colony, nutrients requirements increase as R^2. The diffusive uptake only increases as R, implying the existence of a diffusional *bottleneck* where nutrient requirements will exceed influx. **(b)** The flow around the organism results in an enhancement of uptake producing an effective scaling with R^2 thereby mitigating the diffusive limitations on uptake.

Given genetic similarity of these species and the regularity of their life-cycle, the volvocales constitute a family of organisms where nutrient needs can be compared between species in a meaningful manner. On dimensional grounds, these nutrient requirements must scale with the number of cells and will therefore be proportional to R^2. However, from the previous section we know that the diffusive flux into a sphere scales as $D\rho_0/R$, so the total uptake from diffusion would only scale as R. This suggests that metabolic demands will outgrow nutrient influx as the organism size increases, implying that there exists a *bottleneck* radius R_b beyond which diffusion alone is no longer sufficient to meet the nutrient requirements of the organism (fig 1.4a). Estimates for this radius depend on a number of poorly known factors, but would lie somewhere around $R_b = 50 - 200$ μm (Short et al., 2006).

It turns out that this diffusional bottleneck is mitigated by the increased Péclet number of the flow around the organism. A typical Péclet number can be calculated for each species in terms of the force per unit area f that results from the flagellar beating. Since beating frequencies, flagella lengths and cell spacing are similar across species, this force can be taken as constant. The swimming velocity then shows an approximate scaling (Short et al., 2006)

$$V \simeq \frac{\pi f R}{8\eta} \,. \tag{1.15}$$

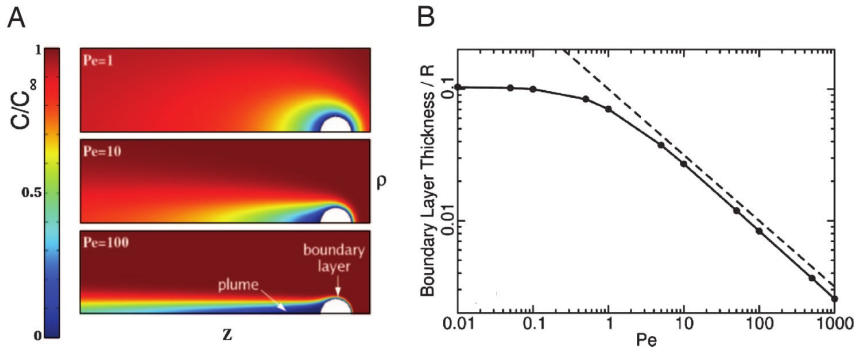

Figure 1.5 Scaling of the diffusive boundary layer with the Péclet number as presented in (Short et al., 2006). **(a)** As the Péclet number increases, the steady-state concentration profile develops a thin boundary layer at the leading edge of the organism. A depleted plume trails on the other side. **(b)** The typical size of the boundary layer δ at the leading edge shows an asymptotic scaling with the Péclet number $\delta \sim \mathrm{Pe}^{-1/2}$.

The Péclet number of the flow therefore scales as

$$\mathrm{Pe} = \frac{RV}{D} = \frac{fR^2}{8\eta D} = \left(\frac{R}{R_a}\right)^2 , \qquad R_a = \sqrt{\frac{8\eta D}{\pi f}} . \tag{1.16}$$

Here the *advective radius* R_a defines the organism size at which Pe = 1. Its typical value lies somewhere around $R_a \sim 10$ μm, indicating that Pe > 1 for all species in the volvocalean family, reaching values Pe = 200 − 300 for larger species such as *Volvox Carteri* (Solari et al., 2006).

Nutrient uptake in the presence of this flow is precisely described by the spherical problem we introduced for *E. coli* in the previous section. Here the flow field can be solved from the boundary condition in the shear stress $\sigma_{r\theta} = f$ (Short et al., 2006). A finite element method can then be used to calculate the steady-state concentration profile around the organism, assuming a perfect sink at the surface (fig 1.5). In the absence of flow, the concentration profile will be given by equation (1.9). As the Péclet number increases this profile becomes asymmetrical (fig 1.5a). At the leading edge of the organism a boundary layer develops as a result of the fact that the flow advects nutrient rich material towards the surface of the cell. A depleted plume trails behind the organism.

The typical width δ of the boundary layer decreases with the Péclet number. Since the flux is given by the gradient of the concentration $F = -D\nabla\rho$, the decrease in boundary layer size increases the rate of uptake as

$F \sim 1/\delta$. Finite element analysis (fig 1.5b) reveals that in the asymptotic regime $Pe \gg 1$, the boundary layer size exhibits a scaling

$$\delta \sim Pe^{-1/2} . \tag{1.17}$$

Given that $Pe \sim (R/R_a)^2$ the typical flux thus depends on the organism size as

$$F \sim 1/\delta \sim (R/R_a) . \tag{1.18}$$

The total flux into the cell is given by the integral of the flux over the surface. So if this boundary layer scaling were to extend all the way around the organism, the total 'current' into the cell would show a $I \sim R^3$ dependence. As it turns out full numerical analysis show that the average flux levels off a large Péclet numbers, presumably because the effective surface area covered by the boundary layer scales as R. However, this scaling is 'good enough' in the sense that the total current scales as $I \sim R^2$ (fig 1.4b) thereby removing the diffusional bottleneck as long as $R_b > R_a$.

So we see that in the case of *Volvox*, an organism living a *life at high Péclet numbers* can use swimming to enhance diffusive uptake. Since the Reynolds number of these flows is still quite low, this effect has nothing to do with an enhancement of mixing. Instead it is based purely on a scaling of the typical concentration gradients around the organism due to advection.

It is this type of effect that may well play a role in cytoplasmic streaming. Since cell sizes of organisms exhibiting streaming are typically larger than 100 μm and the velocities are often of order 10 μm or higher, the Péclet numbers associated with these flows would be order 1, or possibly much larger when considering diffusion of structures such as proteins in crowded cellular environments. Thus if internal circulation does indeed help mitigate the limitations of diffusion in large cells, it may be by inducing a change in the typical boundary layer size around metabolically active structures. It is this notion that we will explore further in chapters 3 and 4.

Our work in this context will focus on the characean algae. Not only are these species the best studied example of organisms exhibiting streaming, but the cylindrical geometry of the internodal cells is well suited to hydrodynamic analysis.

To identify what role streaming could play in enhancing metabolic rates in characean algae, we will begin this thesis with a discussion of the research performed on these organisms over the past decades. In the third

chapter we will present a hydrodynamic solution of the flow field inside characean internodes. The effects of this flow on diffusive transport will be discussed in the chapter that follows. Finally we will present measurements based on NMR spectroscopy and tracer particle injection. We conclude with an overview of our findings and a discussion of future directions of research.